(NASA-CR-164141) CONTINUED ANALYSIS OF OSO-8 AND KITT PEAK DATA ON SOLAR FACULAE Final Technical Report, 1 Jun. 1978 - 30 Nov. 1979 (California State Univ., Northridge.) 125 p HC A06/MF A01 CSCL 03B G3/92

N81-21991

Unclas 41829

FINAL TECHNICAL REPORT

NASA Grant No. NSG-7456

Title: Continued Analysis of OSO-8 and Kitt Peak Data on Solar Faculae

Prepared by G. A. Chapman
Calif. State Univ.
CSU, Northridge, Foundation
18111 Nordhoff St.
Northridge, CA 91330

Performing Period 6/01/78 to 11/30/79

April 1981

Gary A. Chapman

Gary A. Chapman
Principal Investigator

Final Technical Report for NASA Grant No. NSG-7456

I. Introduction

The purpose of this research was to study the magnetic, velocity, and brightness structure of solar faculae in conjunction with the LPSP - team of the OSO-8 satellite. The research involved improved facular models and analysis of spacecraft and groundbased data. As part of this research, a trip was made to France by the PI for the purpose of continuing the data analysis at the Observatoire de Paris, Meudon. The research under this grant has proceeded along two directions:

(a) the improvement of semi-empirical models of faculae to determine the strength and shape of the magnetic field and

(b) the development of an improved data base, including space-and ground-based data, to improve facular models.

II. Facular Models

An improved facular model is presented as Appendix A. This model is based primarily on spectral data using mostly weak (20 - 65 mA Eq. W.) Fraunhofer lines. The model, 7B14/HSRASP, shows a large temperature excess in the upper layers, near the height of the limb, of 800K and a magnetic field strength of 411 gauss. The temperature in the facular flux tube becomes less than that in the photosphere at a depth of -100km and this temperature deficit increases with depth to about -3800K at a depth of 100km below $\tau_{5000} = 1$ in the quiet sun. The cross-sectional area of the flux tube increases with height. The diameter given in Table 3 of Appendix A was determined from pressure balance, $\Delta P = B^2/8\pi$, and neglect of the change in angle of the field lines as they diverge upwards. Subsequent calculations, not yet completed, show that only the geometry in the highest layers are affected (and then not too greatly) when allowance is made for the curvature of the magnetic field lines. The effect of including the angle of

divergence of the field lines is that the flux tube must remain of smaller cross-section and thus not diverge so rapidly compared to the case of simple $B^2/8\pi$ pressure balance. In other words, the effects of magnetic tension are such that the flux tube must be made more uniform with height in order to insure pressure equilibrium. For example, for the model 7B14/HSRASP, the radius of the flux tube without regard for tension forces is about 450km at a height of 600km. Correcting this radius for tension forces causes the radius to decrease to about 300km at the same height. At a height of 200km the change is only about 10km in a radius of 120km or about an 8% decrease.

A cross-section of this model is shown in Figure 1. The solid line is the result of ignoring tension forces and is given by $B^2/8\pi = P_{ext} - P_{int}$, where P_{ext} and P_{int} are the external and internal gas pressures, respectively. The smaller cross-section with the long dashes is the result of 10 iterations on the magnetic flux density, including tension forces. We assume that $B_Z \neq f(r)$ and $B_r \propto r \frac{\partial B}{\partial Z}$. At each iteration the shape of the flux tube was fitted to a polynomial and for a chosen flux the equations of Dicke (eq. 22, 1970) were used to modify the magnetic field to achieve a flux tube shape more nearly in pressure equilibrium. The relation used was

$$\langle \delta P \rangle = - \frac{1}{8\pi} \langle B_Z^2 + r \frac{\partial}{\partial Z} (B_r B_Z) \rangle .$$

The brackets indicate averages over the cross section of the flux tube. Since these tubes deviate only slowly from right circular cylinders, the material density was obtained from hydrostatic equilibrium.

Appendix B shows the section of the computer program that implements the above procedure. The future pursuit of this problem should make use of possible non-hydrostatic models, provided further constraints or boundary conditions can be found from observations.

III. OSO-8 Data Reduction

This part of the project has not been completed. We are waiting for further data reduction of OSO-8 data from the LPSP experiment. A paper has been prepared based on the ground-based magnetograms obtained at Kitt Peak National Observatory (Appendix B). A small but useable set of spacecraft data was identified during my 1978 visit to France, but funding and personnel problems have hindered the completion of data reduction.

It is hoped that at some print in the future the analysis of the selected OSO-8 data can be completed. We will attempt to obtain quantitative correlations between the intensity at various wavelengths in the MgII h and k and CaII H and K lines with magnetic flux from the KPNO data.

IV. Ground-based data on Faculae

We also need information on continuum radiation losses. For this we have used data from an Extreme Limb Photometer at the San Fernando Observatory. This data was limited to large angles from the vertical so we do not have complete coverage of the continuum radiation field. In order to separate out the effects of sunspots these were studied near the center of the disk and the data presented by sunspot area. The preliminary results have been published as changes in the solar constant in Ap. J. 242. It was found that faculae near the limb produced an excess brightness of $3\text{-}4 \times 10^{-2}$ averaged over the plage area and sunspots produced a decrease of 62% over the sunspot area. This data can be used later to compare with the magnetic flux of the corresponding active region to look for a correlation with magnetic flux.

PAPERS SUPPORTED IN PART BY THIS GRANT

Chapman, G. A. 1979, Ap. J. 232, 923. "New Models of Solar Faculae".

Chapman, G. A. 1980, Ap. J. (Letters), 242, L45. "Variations in the Solar Constant Due to Solar Active Regions".

Mouradian, Z., Chapman, G., Dumont, S. Fang, C, Feng, Y., and Pecker, J. E. 1981, Proceedings of the Japan-France Seminar on Solar Physics, p.p. 121-124.

Pecker, J. E., Dumont, S., Mouradian, Z., and Chapman, G. 1978. OSO-8 Workshop, Boulder, CO, "The Establishment of a Facular Model from the Photoshpere to the Corona: Morphological Aspect, p.p. 172-182.

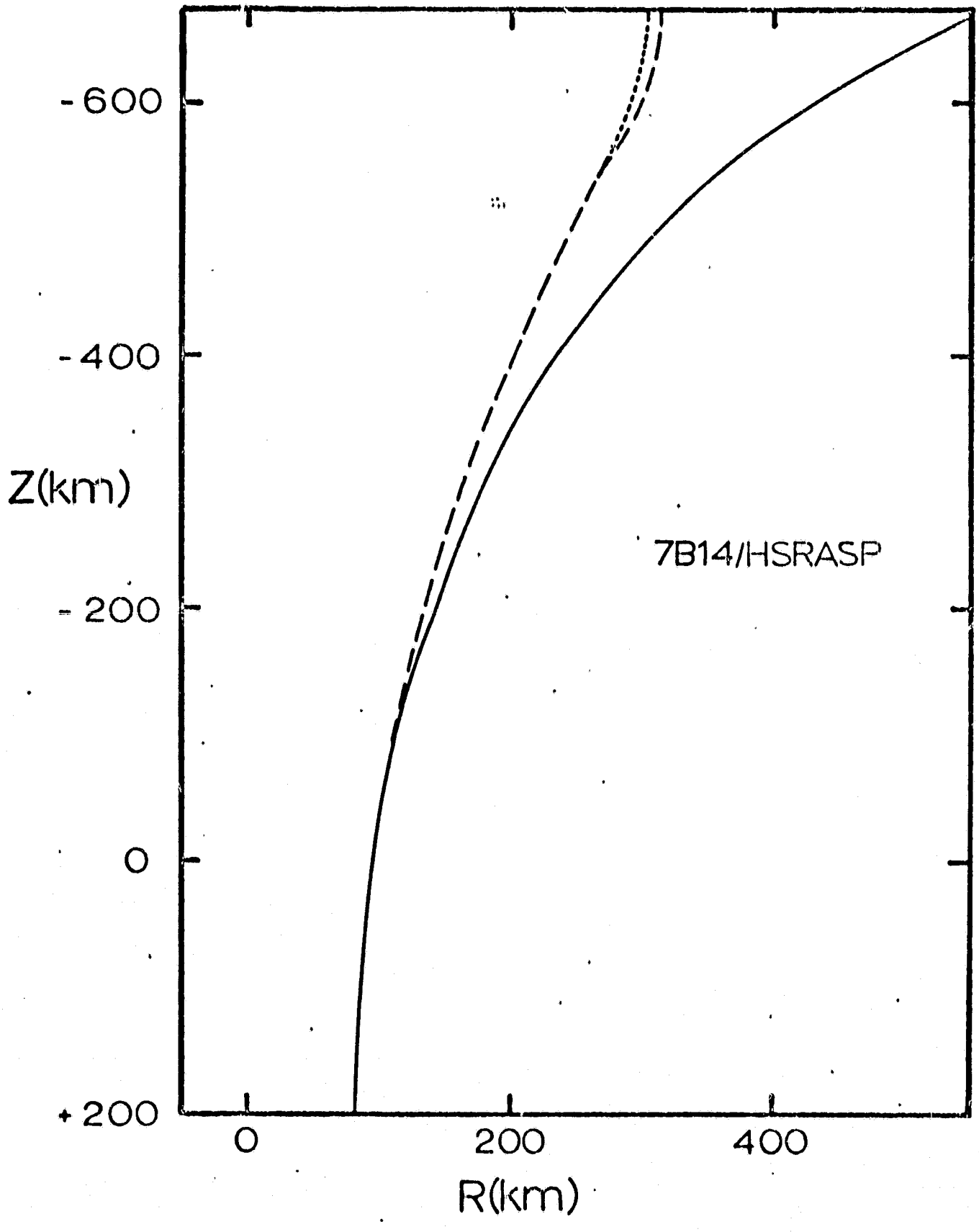

Fig. 1

Appendix A

THE ASTROPHYSICAL JOURNAL, 232:923–928, 1979 September 15

NEW MODELS OF SOLAR FACULAE

G. A. CHAPMAN
San Fernando Observatory and Department of Physics and Astronomy, California State University, Northridge
Received 1977 June 13; accepted 1979 March 21

ABSTRACT

A new semiempirical model of photospheric faculae is presented in tabular form. In an earlier paper (Chapman) a preliminary version of this model was used to construct line profiles that were compared with observations. The magnetic field is estimated from horizontal pressure equilibrium without tension forces. The geometry of the flux tube is determined from this estimated magnetic field and an assumed flux of 4.4×10^{17} gauss cm^2. The model is discussed in relation to recent observations.

Subject headings: Sun: atmosphere — Sun: faculae — Sun: magnetic fields

I. INTRODUCTION

A number of semiempirical models of solar faculae have been constructed which incorporate certain improvements over earlier models (Chapman 1970). For example, the model from the 1970 paper did not include the effects of a magnetic field in the horizontal pressure balance, whereas newer models have a vertically varying magnetic field to achieve pressure balance.

There is considerable evidence that the magnetic field has a horizontal scale comparable to the filigree and is probably cospatial with the thermal perturbation. Much of this evidence was reviewed by Harvey (1977). In their recent analysis, Tarbell and Title (1977) indicated that filigree and the small-scale magnetic field are cospatial to within less than 1″. Spectra presented by Koutchmy and Stellmacher (1978) support this correlation, although the authors argue that the brightness-magnetic field correlation may not be good at the sub-arcsec level.

Parker (1976) demonstrated that only a cooling of the gas in the flux tube can result in confinement of the field to the currently accepted value of about 1.5 kilogauss (150 mT). This cooling could come about by blocking of heat transport across magnetic field lines as argued by Spruit (1977) or by generation of MHD waves as proposed by Parker (1974). The use of von Zeipel's theorem by Dicke (1970) led him to a formalism in which there is a strong relation between the temperature excess (or deficit) and the topology of the magnetic field.

The model presented here is a refinement and extension of the one used in Chapman (1977) and labeled 7B13/HSRA. This model was based on line profile measurements to a much greater extent than the earlier 1970 model. In addition, the effect of a strong magnetic field and its variation with height were used in calculating line profiles. In this paper we wish to discuss this model in more detail and to point out possible improvements. In § II we present the models and some of the assumptions used in them. In § III we discuss limitations in and possible improvements to the model 7B14/HSRASP.

II. PRESENTATION OF RESULTS

Facular models are developed from a photospheric model. The photospheric model used here is an extension of the HSRA (Gingerich *et al.* 1971) made by matching the convection-zone model of Spruit (1974) at the $\tau_{5000\,\text{Å}} = 2$ level. We require a photospheric model that goes beyond the depth of the HSRA model because of the downward shifts of the facular model with respect to the photosphere required for pressure balancing. This extended model, which goes to $\tau_{5000} = 500$ ($Z = 255$ km), is referred to as the HSRASP. That part which differs from the HSRA is given in Table 1.

Facular models are defined by a ΔT versus $\tau_{5000\,\text{Å}}$ relation, where $\Delta T = T_{\text{facular}} - T_{\text{photosphere}}$. This relation must be determined by trial and error since the details of energy transport are unknown. Figure 1 gives the T versus τ relation for the HSRA, Spruit's convection zone, and several facular models. Also shown are two crude intergranular lane models made without regard to kinematics. Table 2 gives the actual values of temperature used in constructing facular model 7B14/HSRASP.

Given a T versus τ relation, a facular model is formed by integrating the equation of hydrostatic equilibrium downward from $\tau_{5000\,\text{Å}} = 10^{-5}$. The opacity is due to H^- and atomic hydrogen as given by the computer codes of Carbon and Gingerich (1969). The equation of state is given by computer codes from Mihalas (1967) and made available by Dr. J. Heasley. Before integrating the facular model, the facular and photospheric models are interpolated onto a scale uniform in 0.05 log τ so that each model will have 155 levels. This degree of fineness helps in later ray-tracing.

After the facular model is generated on a τ-scale in common with that of the photosphere, we must change the basis from optical depth to geometrical depth and

TABLE 1

DOWNWARD EXTENSION OF QUIET SUN, HSRASP

τ	T	P	PE	κ	ρ	Z
1.584893	6860.0	1.472E+05	1.419E+02	1.39E+00	3.34E−07	1.80E+06
1.995262	7140.0	1.540E+05	2.345E+02	2.02E+00	3.35E−07	2.83E+06
2.511886	7501.8	1.596E+05	4.257E+02	3.16E+00	3.29E−07	3.44E+06
3.162278	7808.2	1.642E+05	6.792E+02	4.54E+00	3.25E−07	3.96E+06
3.981072	8056.3	1.684E+05	9.707E+02	6.04E+00	3.23E−07	4.43E+06
5.011872	8265.3	1.725E+05	1.295E+03	7.65E+00	3.22E−07	4.90E+06
6.309573	8447.0	1.767E+05	1.648E+03	9.38E+00	3.22E−07	5.37E+06
7.943282	8611.4	1.810E+05	2.036E+03	1.13E+01	3.23E−07	5.86E+06
10.000000	8763.7	1.856E+05	2.463E+03	1.33E+01	3.25E−07	6.38E+06
12.589254	8908.4	1.906E+05	2.940E+03	1.56E+01	3.27E−07	6.93E+06
15.848932	9046.3	1.958E+05	3.467E+03	1.82E+01	3.30E−07	7.52E+06
19.952623	9180.4	2.016E+05	4.056E+03	2.11E+01	3.34E−07	8.15E+06
25.118864	9316.3	2.079E+05	4.722E+03	2.44E+01	3.39E−07	8.83E+06
31.622777	9452.5	2.148E+05	5.468E+03	2.81E+01	3.44E−07	9.58E+06
39.810717	9576.6	2.223E+05	6.281E+03	3.21E+01	3.50E−07	1.04E+07
50.118723	9691.0	2.302E+05	7.178E+03	3.67E+01	3.57E−07	1.12E+07
63.095734	9826.6	2.395E+05	8.235E+03	4.21E+01	3.66E−07	1.21E+07
79.432823	9947.0	2.493E+05	9.382E+03	4.80E+01	3.75E−07	1.31E+07
100.000000	10059.0	2.600E+05	1.065E+04	5.46E+01	3.85E−07	1.41E+07
125.892541	10186.0	2.722E+05	1.211E+04	6.21E+01	3.97E−07	1.53E+07
158.489319	10299.0	2.853E+05	1.369E+04	7.05E+01	4.10E−07	1.64E+07
199.526231	10424.0	3.003E+05	1.554E+04	8.01E+01	4.24E−07	1.78E+07
251.188643	10546.0	3.167E+05	1.760E+04	9.11E+01	4.40E−07	1.91E+07
316.227766	10673.0	3.349E+05	2.000E+04	1.04E+02	4.58E−07	2.06E+07
398.107171	10804.0	3.550E+05	2.275E+04	1.18E+02	4.78E−07	2.22E+07
501.187234	10935.0	3.772E+05	2.583E+04	1.35E+02	5.00E−07	2.38E+07

NOTE.—The units used are cgs with τ (optical depth) at 5000 Å, T (temperature), P (pressure), PE (electron pressure), ρ (mass density), and Z (geometrical depth).

shift the facular model downward to obtain horizontal pressure balance. The minimum shift is introduced so as to keep the facular gas pressure at each depth less than the corresponding photospheric gas pressure. The pressure difference gives a preliminary estimate of the magnetic field through

$$B = [8\pi(P_{ph} - P_f)]^{1/2}.$$

The temperature difference, $\Delta T(Z) = T_f(Z) - T_{ph}(Z)$, on a depth scale is also determined. The shape of the flux tube is defined by the assumed magnetic flux ϕ and

$$R(Z) = \left[\frac{\phi}{\pi B(Z)}\right]^{1/2}.$$

This relation neglects the spreading with height of the magnetic flux tube. Except for the upper levels, the error in tube radius caused by this last assumption is quite small. We have adopted $\phi = 4.4 \times 10^{17}$ gauss cm^2 (Mehltretter 1974).

For most models investigated, vertical shifts of about 150 km downward at $\tau_{0.5\mu m} = 1$ are required to have the internal gas pressure less than the external. This shift corresponds to a Wilson depression in sunspot models and is present in the models of Spruit (1976). The magnetic field strength at $Z = 0$ ($\tau_{0.5}^{ph} = 1$) is typically near 1500 gauss.

Table 3 presents the facular model 7B14/HSRASP, which is essentially the same as facular model 7B13/HSRA given in Chapman (1977) but extended to greater geometric depth.

We have experimented with other models for the photosphere to determine the effect on deduced magnetic field strength. An extreme variant on the photosphere might be an intergranular lane. We have generated a facular model from an intergranular

TABLE 2

T VERSUS $\log_{10} \tau_{5000}$, 10 STEPS PER DECADE FOR FAC MOD 7B14/HSRASP

$\log_{10}\tau$	−0.9	0.8	0.7	0.6	0.5	0.4	0.3	0.2	0.1	0.0
−5.0	...	...	...	...	...	...	...	...	...	6170
−4.0	6136	6101	6067	6033	5999	5965	5931	5897	5863	5829
−3.0	5794	5760	5726	5692	5658	5624	5590	5556	5522	5487
−2.0	5453	5419	5385	5351	5317	5307	5321	5336	5350	5364
−1.0	5379	5393	5407	5421	5436	5450	5464	5479	5493	5520
0.0	5560	5600	5640	5680	5760	5840	5920	6000	6080	6205
+1.0	6410	6640	7070	7580	7980	8380	8780	9180	9580	9980
+2.0	10380	10780	11180	11302	11424	11546	11668	11790	11912	12034
+3.0	12156	12278	12400	12522	12644	12766	12888	...	...	...

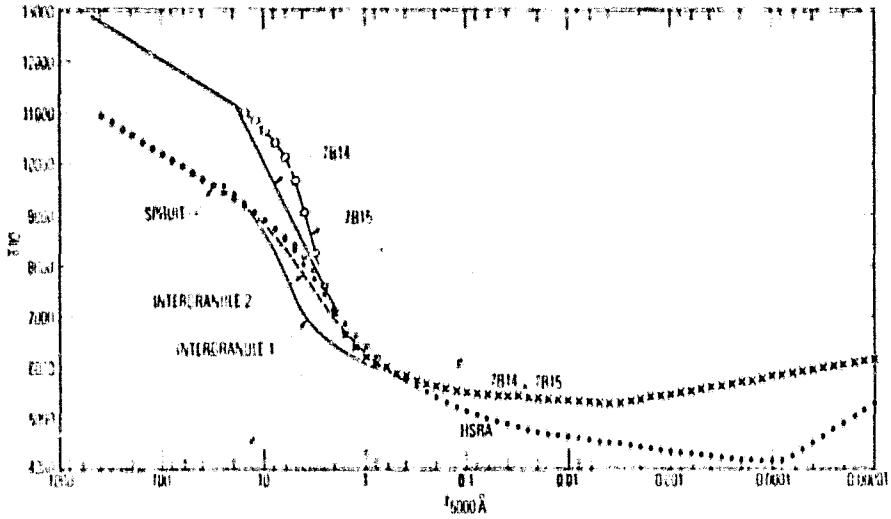

FIG. 1.—Temperature versus optical depth at 5000 Å. The convection-zone model of Spruit is joined at $\tau = 2$ to the HSRA and the combined photospheric model is called HSRASP (see Table 1). The facular model 7B14 is eventually placed on a common depth scale with the HSRASP and the depth scales shifted relative to each other (see Table 3).

region model called INGRAN 2 which has a contrast, with respect to the HSRA, of -10% at disk center falling to zero contrast for $\mu = \cos\theta \leq 0.3$.

The magnetic field and temperature excess for facular model 7B14/INGRAN 2 are less than for the models of Table 3 derived from the HSRA. For example, the magnetic field strength at $Z = 0$ is 1340 gauss and the temperature excess at $z \approx -315$ km, the approximate "height of the limb," is about 709 K compared to 1511 gauss and 760 K, respectively, for facular model 7B14/HSRASP.

We confirm the importance of the "hot wall" effect described by Spruit (1976) to the continuum contrast of faculae. This effect ascribes the excess brightness of faculae near the limb to the enhanced visibility of the deeper (hence hotter) layers of the photosphere seen through the optically thin flux tubes. The flux tubes are optically thin because of the lower mass density which is required by horizontal pressure balance. However, the "hot wall" at the edge of the flux tube cannot be seen very near the limb because of geometrical foreshortening. Hence continuum limb darkening evidence for the existence of a temperature enhancement in the upper levels of faculae may depend critically on the contrast in the region $0.2 < \mu \leq 0$.

III. DISCUSSION

These facular models have the general characteristics described by Parker (1976) and by Spruit (1976), namely, that the magnetic field is confined by a deficit in the gas pressure which is itself caused by a temperature deficit in the deeper layers. An understanding of how this condition is brought about is not yet within our grasp. Two alternate explanations are cooling by wave generation (Parker 1976; Roberts 1976) and blocking of heat flow (Spruit 1977). We need more data in order to test these two hypotheses.

The temperature deficit in the deeper layers should be observable as darker-than-average features at 1.64 μm. Worden (1975) has reported evidence for a 50–500 K temperature deficit in facular structures in observations at this wavelength. The temperature range indicates the uncertainty in corrections caused by low spatial resolution.

It has been suggested (Chapman 1974) that for sufficiently large flux, about 4×10^{18} to 6×10^{18} gauss cm^2, the magnetic structure begins to behave more like a pore than a facula. Below this flux boundary, facular structure may not depend strongly on magnetic flux. This behavior is supported by observations of Frazier (1978) which show that the excess brightness flux in the core of the 5250.2 Å line is linearly related to the measured magnetic flux up to magnetic flux levels of 40 GWb (4×10^{18} maxwells).

On the other hand, Spruit (1977) has presented evidence which suggests that faculae vary in structure according to their size (used as a measure of flux). Better observations are needed which can accurately measure the magnetic flux of individual flux tubes.

These facular models are not structurally self-consistent because magnetic tension forces have not been included. We are attempting to determine the influence for simple flux-tube configurations. The formalism is adapted from Dicke (1970), who shows from von Zeipel's theorem that magnetic and velocity stresses in the photosphere will lead to perturbations in the pressure, density, and temperature. We will include the effect of steady flows such as that given by Giovanelli and Slaughter (1978). However, we will require much better knowledge of boundary conditions before we can hope to obtain the true shape of the field in a self-consistent model.

There has been some discussion of the need for two-dimensional radiative transfer in calculating emergent intensities. Stenholm and Stenflo (1977) have shown

TABLE 3

FACULAR MODEL 7B14/HSRASP

τ	T	P	PE	κ	ρ	Z	$T-TP$	Mapfield	Diameter
2.00E−05.....	6.07E+03	6.49E+01	5.38E−01	1.43E−02	1.05E−10	−8.32E+07	+ 767	8.7	2.54E+08
2.73E−05.....	6.02E+03	7.93E+01	5.35E−01	1.36E−02	2.04E−10	−8.03E+07	+ 850	20.8	1.64E+08
4.00E−05.....	5.96E+03	1.06E+02	5.40E−01	1.28E−02	2.75E−10	−7.63E+07	+ 924	27.0	1.44E+08
5.67E−05.....	5.91E+03	1.42E+02	5.54E−01	1.23E−02	3.75E−10	−7.22E+07	+ 1003	33.4	1.29E+08
7.57E−05.....	5.87E+03	1.85E+02	5.67E−01	1.22E−02	4.85E−10	−6.85E+07	+ 1080	41.9	1.16E+08
9.58E−05.....	5.84E+03	2.29E+02	5.84E−01	1.24E−02	6.11E−10	−6.55E+07	+ 1175	52.1	1.04E+08
1.17E−04.....	5.81E+03	2.76E+02	5.95E−01	1.26E−02	7.38E−10	−6.30E+07	+ 1275	62.6	9.46E+07
1.39E−04.....	5.78E+03	3.24E+02	6.06E−01	1.28E−02	8.71E−10	−6.08E+07	+ 1379	72.1	8.82E+07
1.62E−04.....	5.76E+03	3.73E+02	6.16E−01	1.30E−02	1.01E−09	−5.89E+07	+ 1477	81.1	8.31E+07
1.85E−04.....	5.74E+03	4.20E+02	6.25E−01	1.32E−02	1.14E−09	−5.73E+07	+ 1537	90.4	7.87E+07
2.08E−04.....	5.72E+03	4.68E+02	6.32E−01	1.34E−02	1.27E−09	−5.58E+07	+ 1550	100.3	7.47E+07
2.34E−04.....	5.70E+03	5.20E+02	6.40E−01	1.36E−02	1.42E−09	−5.44E+07	+ 1528	110.6	7.12E+07
2.62E−04.....	5.69E+03	5.78E+02	6.47E−01	1.38E−02	1.58E−09	−5.30E+07	+ 1495	121.2	6.80E+07
2.95E−04.....	5.67E+03	6.42E+02	6.55E−01	1.40E−02	1.76E−09	−5.16E+07	+ 1463	132.4	6.50E+07
3.31E−04.....	5.65E+03	7.12E+02	6.63E−01	1.42E−02	1.96E−09	−5.02E+07	+ 1426	144.3	6.23E+07
3.71E−04.....	5.63E+03	7.89E+02	6.71E−01	1.45E−02	2.18E−09	−4.89E+07	+ 1384	156.8	5.98E+07
4.16E−04.....	5.62E+03	8.73E+02	6.78E−01	1.47E−02	2.42E−09	−4.75E+07	+ 1337	170.2	5.74E+07
4.68E−04.....	5.60E+03	9.68E+02	6.86E−01	1.50E−02	2.69E−09	−4.62E+07	+ 1295	184.2	5.51E+07
5.26E−04.....	5.58E+03	1.07E+03	6.95E−01	1.53E−02	2.99E−09	−4.48E+07	+ 1253	199.1	5.30E+07
5.91E−04.....	5.57E+03	1.19E+03	7.03E−01	1.56E−02	3.33E−09	−4.35E+07	+ 1211	214.9	5.11E+07
6.66E−04.....	5.55E+03	1.32E+03	7.12E−01	1.59E−02	3.70E−09	−4.21E+07	+ 1168	231.7	4.92E+07
7.50E−04.....	5.53E+03	1.46E+03	7.22E−01	1.62E−02	4.12E−09	−4.08E+07	+ 1126	249.6	4.74E+07
8.46E−04.....	5.51E+03	1.62E+03	7.31E−01	1.65E−02	4.59E−09	−3.94E+07	+ 1082	268.7	4.57E+07
9.55E−04.....	5.49E+03	1.80E+03	7.41E−01	1.69E−02	5.11E−09	−3.80E+07	+ 1034	288.9	4.40E+07
1.08E−03.....	5.48E+03	2.00E+03	7.51E−01	1.74E−02	5.70E−09	−3.67E+07	+ 985	310.4	4.25E+07
1.23E−03.....	5.46E+03	2.23E+03	7.64E−01	1.78E−02	6.36E−09	−3.53E+07	+ 932	333.3	4.10E+07
1.39E−03.....	5.44E+03	2.48E+03	7.77E−01	1.83E−02	7.11E−09	−3.39E+07	+ 888	357.6	3.96E+07
1.59E−03.....	5.42E+03	2.77E+03	7.91E−01	1.89E−02	7.95E−09	−3.26E+07	+ 844	383.4	3.82E+07
1.81E−03.....	5.40E+03	3.08E+03	8.07E−01	1.95E−02	8.89E−09	−3.12E+07	+ 800	411.0	3.69E+07
2.07E−03.....	5.38E+03	3.44E+03	8.25E−01	2.01E−02	9.96E−09	−2.98E+07	+ 750	440.3	3.57E+07
2.37E−03.....	5.36E+03	3.84E+03	8.46E−01	2.09E−02	1.12E−08	−2.84E+07	+ 700	471.4	3.45E+07
2.72E−03.....	5.34E+03	4.29E+03	8.67E−01	2.17E−02	1.25E−08	−2.70E+07	+ 649	504.8	3.33E+07
3.13E−03.....	5.32E+03	4.81E+03	8.93E−01	2.26E−02	1.41E−08	−2.56E+07	+ 598	540.1	3.22E+07
3.63E−03.....	5.31E+03	5.39E+03	9.44E−01	2.40E−02	1.58E−08	−2.42E+07	+ 558	577.5	3.11E+07
4.23E−03.....	5.31E+03	6.05E+03	1.02E+00	2.59E−02	1.78E−08	−2.27E+07	+ 519	617.4	3.01E+07
4.96E−03.....	5.32E+03	6.79E+03	1.13E+00	2.84E−02	1.99E−08	−2.13E+07	+ 480	659.9	2.91E+07
5.86E−03.....	5.33E+03	7.62E+03	1.25E+00	3.10E−02	2.23E−08	−1.98E+07	+ 436	705.3	2.82E+07
6.98E−03.....	5.34E+03	8.57E+03	1.38E+00	3.39E−02	2.50E−08	−1.84E+07	+ 392	753.4	2.73E+07
8.38E−03.....	5.35E+03	9.64E+03	1.53E+00	3.72E−02	2.81E−08	−1.69E+07	+ 343	804.3	2.64E+07
1.01E−02.....	5.36E+03	1.09E+04	1.69E+00	4.08E−02	3.16E−08	−1.54E+07	+ 285	858.4	2.55E+07
1.23E−02.....	5.38E+03	1.23E+04	1.88E+00	4.48E−02	3.55E−08	−1.39E+07	+ 217	915.5	2.47E+07

how, for certain non-LTE situations, one can produce an intensity enhancement in the cores of weak lines for flux-tube models having no temperature enhancement. For their intermediate cases about one-fourth to one-third of the observed weak-line contrast was produced. Their results imply that some temperature enhancement is still required to produce observed line weakenings. In any case observations in the wing of the K line (Heasley, Kneer, and Chapman 1977), in the CN bandhead at $\lambda = 3883$ Å, and in the far-infrared (Hudson 1975) strongly support a temperature enhancement for faculae.

Furthermore, Mihalas, Auer, and Mihalas (1978) have shown that horizontal radiative transfer will probably not lead to intensity enhancements for an embedded flux tube, but rather the atmosphere will achieve some kind of radiative average. The emergent intensity will then be composed of contributions from each part of the atmosphere, depending on the geometry of the flux tube and the line of sight.

We have assumed that the brightness and magnetic field of a facula are cospatial. A spectrum of a facula (Fig. 12 of Koutchmy and Stellmacher 1978) showed that, although the intensity variation and magnetic field strength were not exactly correlated within the facula, their boundaries correlated quite well. The similarity between the intensity and magnetic contours is more impressive than the difference. This spectrum also showed no evidence for a velocity in the facula, although considerable evidence exists for velocities in some faculae (Harvey 1977).

We believe that faculae and filigree are basically the same phenomenon but seen at different parts of the disk. This view is supported by observations from Sacramento Peak Observatory (1977 August), which show the spatial similarity near the limb between filigree and faculae. We believe that the morphological differences between filigree far from the limb and faculae near the limb, discussed by Muller (1975, 1977), are due simply to geometry.

The facular model presented here is intended as a tool to help in understanding small-scale magnetic fields. It may be a guide in the search for a proper physical treatment of flux tubes, but it is not meant to

TABLE 3 *Continued*

τ	T	P	PE	κ	ρ	Z	$T-TP$	Magfield	Diameter
1.50E−02	5.39E+03	1.38E+04	2.02E+00	4.92E−02	4.00E−08	−1.23E+07	+150	975.6	2.40E+07
1.83E−02	5.40E+03	1.56E+04	2.32E+00	5.40E−02	4.80E−08	−1.08E+07	+72	1038.6	2.32E+07
2.24E−02	5.41E+03	1.76E+04	2.57E+00	5.93E−02	5.06E−08	−9.30E+06	−16	1103.8	2.25E+07
2.74E−02	5.43E+03	1.98E+04	2.86E+00	6.52E−02	5.68E−08	−7.80E+06	−113	1170.3	2.19E+07
3.34E−02	5.44E+03	2.22E+04	3.17E+00	7.18E−02	6.36E−08	−6.33E+06	−211	1237.0	2.13E+07
4.06E−02	5.45E+03	2.48E+04	3.49E+00	7.81E−02	7.09E−08	−4.91E+06	−314	1303.5	2.07E+07
4.88E−02	5.46E+03	2.76E+04	3.83E+00	8.50E−02	7.87E−08	−3.55E+06	−428	1368.2	2.02E+07
5.82E−02	5.47E+03	3.05E+04	4.19E+00	9.22E−02	8.68E−08	−2.27E+06	−561	1431.0	1.98E+07
6.85E−02	5.48E+03	3.34E+04	4.55E+00	9.92E−02	9.50E−08	−1.08E+06	−716	1489.1	1.94E+07
7.95E−02	5.49E+03	3.64E+04	4.90E+00	1.06E−01	1.03E−07	0	−897	1541.9	1.91E+07
9.09E−02	5.51E+03	3.92E+04	5.29E+00	1.13E−01	1.11E−07	+9.68E+05	−1103	1587.3	1.88E+07
1.02E−01	5.52E+03	4.19E+04	5.69E+00	1.20E−01	1.18E−07	+1.82E+06	−1337	1626.6	1.86E+07
1.13E−01	5.54E+03	4.43E+04	6.08E+00	1.27E−01	1.25E−07	+2.55E+06	−1600	1660.0	1.84E+07
1.23E−01	5.56E+03	4.64E+04	6.45E+00	1.34E−01	1.30E−07	+3.16E+06	−1945	1685.7	1.82E+07
1.33E−01	5.57E+03	4.84E+04	6.78E+00	1.40E−01	1.35E−07	+3.69E+06	−2239	1705.7	1.81E+07
1.42E−01	5.58E+03	5.02E+04	7.09E+00	1.45E−01	1.40E−07	+4.17E+06	−2475	1723.1	1.80E+07
1.52E−01	5.59E+03	5.20E+04	7.40E+00	1.50E−01	1.45E−07	+4.64E+06	−2672	1740.3	1.79E+07
1.63E−01	5.60E+03	5.39E+04	7.73E+00	1.55E−01	1.50E−07	+5.11E+06	−2842	1756.5	1.79E+07
1.75E−01	5.62E+03	5.59E+04	8.10E+00	1.61E−01	1.55E−07	+5.61E+06	−2995	1772.6	1.78E+07
1.88E−01	5.63E+03	5.82E+04	8.50E+00	1.67E−01	1.61E−07	+6.13E+06	−3134	1789.0	1.77E+07
2.03E−01	5.64E+03	6.07E+04	8.94E+00	1.74E−01	1.68E−07	+6.68E+06	−3265	1806.6	1.76E+07
2.21E−01	5.66E+03	6.34E+04	9.42E+00	1.82E−01	1.75E−07	+7.26E+06	−3390	1823.9	1.75E+07
2.42E−01	5.67E+03	6.65E+04	9.99E+00	1.92E−01	1.83E−07	+7.89E+06	−3508	1842.0	1.74E+07
2.68E−01	5.70E+03	7.00E+04	1.08E+01	2.03E−01	1.92E−07	+8.57E+06	−3618	1861.1	1.73E+07
2.98E−01	5.74E+03	7.39E+04	1.20E+01	2.21E−01	2.01E−07	+9.30E+06	−3715	1881.4	1.73E+07
3.35E−01	5.78E+03	7.84E+04	1.34E+01	2.40E−01	2.12E−07	+1.01E+07	−3796	1901.2	1.72E+07
3.81E−01	5.82E+03	8.33E+04	1.50E+01	2.62E−01	2.23E−07	+1.09E+07	−3867	1921.0	1.71E+07
4.37E−01	5.87E+03	8.90E+04	1.71E+01	2.89E−01	2.37E−07	+1.18E+07	−3954	1944.7	1.70E+07
5.17E−01	5.93E+03	9.56E+04	1.97E+01	3.23E−01	2.52E−07	+1.28E+07	−4020	1964.8	1.69E+07
6.10E−01	5.99E+03	1.03E+05	2.32E+01	3.67E−01	2.70E−07	+1.39E+07	−4071	1983.1	1.68E+07
7.34E−01	6.05E+03	1.13E+05	2.74E+01	4.17E−01	2.90E−07	+1.51E+07	−4135	2005.1	1.67E+07
8.93E−01	6.14E+03	1.22E+05	3.38E+01	4.89E−01	3.11E−07	+1.62E+07	−4163	2026.6	1.66E+07
1.11E+00	6.29E+03	1.33E+05	4.73E+01	6.27E−01	3.28E−07	+1.75E+07	−4132	2051.1	1.65E+07
1.49E+00	6.57E+03	1.46E+05	8.27E+01	9.44E−01	3.45E−07	+1.89E+07	−3981	2069.8	1.65E+07
2.40E+00	7.48E+03	1.62E+05	4.17E+02	3.12E+00	3.36E−07	+2.06E+07	−3194	2086.7	1.64E+07
6.54E+00	9.24E+03	1.75E+05	4.01E+03	2.15E+01	2.87E−07	+2.21E+07	−1560	2126.3	1.62E+07
2.79E+01	1.13E+04	1.83E+05	2.24E+04	1.59E+02	2.20E−07	+2.33E+07	+400	2209.9	1.59E+07

NOTE. The same units as Table 1, where $T - TP$ is the facular-photosphere temperature difference at equal geometric depth, Magfield is the magnetic field strength in gauss, and Diameter is the flux-tube diameter.

be a substitute for a proper physical model. It is not intended that the present model be used above a height of 200 km ($Z \approx -200$ km).

Considerable uncertainty exists concerning the spreading of the magnetic field in the upper layers. The size of the flux tube in these layers will depend on the magnitude of the Wilson depression and the inclusion of tension forces. High-resolution filtergrams in the K line and in the *EUV*, together with magnetic field data for the region of the temperature minimum, could be very helpful in extending facular models toward the chromosphere. Balloon-based observations (Hersé 1977; Hirayama 1978) can help in studying the time-dependent behavior by obtaining long periods of undistorted cinematography. Finally, more work is needed on the energy flow both radiative and non-radiative before satisfactory models of faculae can be constructed.

The author appreciates the contributions of T. Becker, M. Brennan, and M. Gates of the Aerospace Corporation, for providing programming assistance. Dr. James Heasley provided some of the computer codes. Support for this work came from the Aerospace Corporation and from NASA grant NSG-7456.

REFERENCES

Carbon, D. F., and Gingerich, O. 1969, in *Theory and Observations of Normal Stellar Atmospheres* (Cambridge: MIT Press), p. 377.
Chapman, G. A. 1970, *Solar Phys.*, **14**, 315.
———. 1974, *Ap. J.*, **191**, 255.
———. 1977, *Ap. J. Suppl.*, **33**, 35.
Dicke, R. H. 1970, *Ap. J.*, **159**, 25.
Frazier, E. N. 1978, *Astr. Ap.*, **64**, 351.
Gingerich, O., Noyes, R. W., Kalkofen, W., and Cuny, Y. 1971, *Solar Phys.*, **18**, 347.
Giovanelli, R. G., and Slaughter, C. 1978, *Solar Phys.*, **57**, 255.
Harvey, J. W. 1977, in *Highlights of Astronomy*, Vol. 4, ed. E. A. Muller (Dordrecht: Reidel), p. 223.
Heasley, J. N., Kneer, F., and Chapman, G. A. 1977, *Solar Phys.*, **52**, 309.
Hersé, M. 1977, private communication.
Hirayama, T. 1978, *Pub. Astr. Soc. Japan*, **30**, 337.
Hudson, H. S. 1975, *Solar Phys.*, **45**, 69.
Koutchmy, S., and Stellmacher, G. 1978, *Astr. Ap.*, **67**, 93.
Mehltretter, J. P. 1974, *Solar Phys.*, **38**, 43.

Mihalas, D. 1967, in *Methods in Computational Physics*, Vol. 7, ed. B. Alder, S. Fernbach, and M. Rotenberg (New York: Academic), p. 1.
Mihalas, D., Auer, L. H., and Mihalas, B. R. 1978, *Ap. J.*, 220, 1001.
Muller, R. 1975, *Solar Phys.*, 45, 105.
———. 1977, *Solar Phys.*, 52, 249.
Parker, E. N. 1974, *Solar Phys.*, 36, 249.
Parker, E. N. 1976, *Ap. J.*, 204, 259.
Roberts, B. 1976, *Ap. J.*, 204, 268.
Sprutt, H. C. 1974, *Solar Phys.*, 34, 277.
———. 1976, *Solar Phys.*, 50, 269.
———. 1977, *Solar Phys.*, 55, 3.
Stenholm, L. G., and Stenflo, J. O. 1977, *Astr. Ap.*, 58, 273.
Tarbell, T. D., and Title, A. M. 1977, *Solar Phys.*, 52, 13.
Worden, S. P. 1975, *Solar Phys.*, 45, 521.

G. A. CHAPMAN: Department of Physics and Astronomy, California State University, Northridge, 18111 Nordhoff Street, Northridge, CA 91330

```
C
C
C
*DECK FACRST
      SUBROUTINE FACRST(NSTEP,NBASE)
      COMMON/LAB/LABEL(3)
      COMMON/PARAMS/
     * TAUX(100),TX(100),PX(100),PAX(100),DPACX(100),RHOX(100),ZX(100),
     * TAUP(201),TP(201),PP(201),PAP(201),DPACP(201),RHOP(201),ZP(201),
     * TAUI(201),TI(201),PI(201),PEI(201),DPACI(201),RHOI(201),ZI(201),
     * TAU(201),T(201),P(201),PE(201),DPAC(201),RHO(201),Z(201),TTX(100)
      COMMON/PLOTS/IFLAG,XLOOK(100),YCHART(100),
     * CC(13),DD(13),EE(7),GG(3),SS(10)                                 PLOTS-2
      COMMON/TAB1/ET(219),Y(219),THETA(15),PELOG(13),PLOG(13,15),A(5)
      COMMON/TAB2/LIM,IDCK(8),STAR(11),FLAG,WAVLE,FREQ,DAY
      COMMON/TRAN/TITLE(32)
      DIMENSION BFIELD(201),ZZ(201),LAMDAB(201),LAMPR(201)
      DIMENSION XLIMIT(201),XLIMITC(201)
      DIMENSION XSIDE(201)
      DIMENSION RAD(201),RHOT(201),TFB(201),BTOT(201),PMAG(201),OP(201)
      EQUIVALENCE (RAD,PTI),(RHOT,DPACI),(TFB,ZI),(BTOT,KZ),
     . (PMAG,XLIMITC),(OP,XSIMP)
      DIMENSION TAUB(5),ZZ(5,5),DPSTAN(5,2)
      REAL LAMPR
      REAL LAMDAB,KZ
      COMMON/TRANS/FREQX,BFIELD,K,PY
      DIMENSION RTS(11)
      EQUIVALENCE(PE,PI),(LAMPR,RHOI),(XSIMP,TI),(LAMDAB,TAUI)
      DOUBLE PRECISION CP,CI
      COMPLEX RTS
      EXTERNAL ADX
      LOGICAL TEST
      DATA ZZ/25*1.0/
      ZZ(1,2)=-4.0E+7 $ ZZ(2,2)=-3.0E+7 $ ZZ(3,2)=-1.75E+7
      ZZ(4,2)=-5.0E+6 $ ZZ(5,2)=1.5E+7
      DO 815 I=1,5
  815 ZZ(I,1)=1.0
      NOFSET=0
C
C * * * SUFFIX P INDICATES EXPANDED PHOTOSPHERE
C * * * SUFFIX I INDICATES INTERMEDIATE MODIFIED FACULA
C * * * SUFFIXES ARE DROPPED WHEN FINAL FACULAR TERMS ARE FOUND
C
      R=7.0E+10
    5 FORMAT(I10)
    6 FORMAT(1H1)
   10 FORMAT(//)
  910 FORMAT(I3P)
      NSS=NSTEP-1
      TENSOF=0.
      DO 75 N=1,NSS
      TT1=TI(N+1) $ TT=TI(N)
   75 TENSOF=TENSOF+.5*(B(TT1)*EXP(-TAUI(N+1))+B(TT)*EXP(-TAUI(N)))*
     1     (TAUI(N+1)-TAUI(N))
      DELIM=-NBASE/2
      BFLDY=4.4E+17
      BOSTART=100.
      PY=3.1415926
```

Appendix B

ORIGINAL PAGE IS
OF POOR QUALITY

```
      DO 280 J=1,NBASE
      IF(ZI(J)-ZP(1)+1.E-3) 280,282,282
  280 CONTINUE
  282 WRITE(6,5) J
      DO 286 K=1,NBASE
      IF(ZI(J-K+1)-ZP(1)-1.E-3) 288,288,286
  286 CONTINUE
  288 NDELZ=K
      K=NDELZ+NOFSET
      WRITE(6,5) K
      DELZ=ZP(NBASE)-ZP(NBASE-K)
      WRITE(6,291) NDELZ,DELZ
  291 FORMAT(/20X,15H NO. OF STEPS=,I4,5X,11H SHIFT(CM)=,F12.4/)
      DO 292 J=1,NSTEP
  292 ZI(J)=ZI(J)+DELZ
      INDX=1 $ ICHK=1
      DO 330 J=1,NSTEP
      CALL TBLKP(ZP(J),TAU(J),ZI,TAUI,4,INDX,129,6,ICHK,NTEST)
      CALL TBLKP(ZP(J),T(J),ZI,TI,     4,INDX,129,6,ICHK,NTEST)
      CALL TBLKP(ZP(J),P(J),ZI,PI,     4,INDX,129,6,ICHK,NTEST)
      CALL TBLKP(ZP(J),PE(J),ZI,PEI,   4,INDX,129,6,ICHK,NTEST)
      CALL TBLKP(ZP(J),OPAC(J),ZI,OPACI,4,INDX,129,6,ICHK,NTEST)
      CALL TBLKP(ZP(J),RHO(J),ZI,RHOI,4,INDX,129,6,ICHK,NTEST)
  330 Z(J)=ZP(J)
      WRITE(6,341)(TAU(J),T(J),P(J),PE(J),OPAC(J),RHO(J),Z(J),J=1,NSTEP,
     1   2)
  341 FORMAT(1P,7E12.4)
      DO 397 I=1,5
      CALL TBLKP(ZZ(I,2),PTEMP,Z,P,4,INDX,128,6,ICHK,NTEST)
      CALL TBLKP(ZZ(I,2),DPSTAN(I,1),Z,PP,4,INDX,128,6,ICHK,NTEST)
  397 DPSTAN(I,1)=PTEMP-DPSTAN(I,1)
      WRITE(6,341)(DPSTAN(I,1),I=1,5)
      WRITE(6,550)      LABEL
  550 FORMAT(1H1,30X,*FACULAR ATMOS.--FACRST OUTPUT*//30X,8A2/)
      WRITE(6,333)
  333 FORMAT(    4X,4H TAU,8X,2H T,9X,2H P,8X,3H PE,7X,6H KAPPA,6X,4H RH
     1O,8X,2H Z,10X,6H T-TP,6X,9H MAGFIELD,4X,9H DIAMETER,7X,5H STEP/)
C        XLIMIT IS THE FLUX TUBE DIAMETER
      NCOUN=NSTEP+1
      DO 332 K=1,NSTEP
      DELT=T(K)-TP(K)
      DELP=PP(K)-P(K)
      BREM=-1.0
      IF(DELP.LE.0.) GO TO 332
      NCOUN=NCOUN-1
      BREM=(25.12*DELP)**0.5
C        1.1283792 IS SQ. RT. OF 4/PI
      XLIMIT(K)=(BFLUX/BREM)**0.5*1.1283792
      BFIELD(K)=BREM
      IF(K/2*2.EQ.K) GO TO 332
      WRITE(6,29)TAU(K),T(K),P(K),PE(K),OPAC(K),RHO(K),Z(K),DELT,BREM,
     . XLIMIT(K),K
 1003 FORMAT(1P7E11.4)
  332 CONTINUE
   29 FORMAT(8X,1PE10.2,1X,5(E10.2,1X),2X,0PF9.0,5X,F7.1,5X,1PE10.2,7X,
     . I4)
      WRITE(6,5) NCOUN
```

```
      NSB2=NSTEP-2
      NSB3=NSTEP-3
      WRITE(6,204)
  204 FORMAT(/15X,6H DEPTH,5X,9H DIAMETER,9X,35X,5X,12H BCORRECTION)
 1052 FORMAT(3X,I4,1P3E11.3)
 1063 FORMAT(5X,I4,1P2E11.3)
 1074 FORMAT(7X,I4,1P6E11.3)
 1085 FORMAT(9X,I4,1P2E11.3)
      DO 300 N=ICOUN,NSB2
      IF(BFIELD(N).LT.1.E-10) BFIELD(N)=N
      DELTA=Z(N+1)-Z(N)
      CALL DERV(BFIELD,N,DELTA,LAMDAB(N))
  300 LAMDAP(N)=-BFIELD(N)/LAMDAB(N)
      DO 410 I=1,5
      DO 410 J=2,4
  410 ZZ(I,J+1)=ZZ(I,J)*ZZ(I,2)
*  *  *  *  *  *  *  *
      DO 9785 NTRY=1,2
***** **** ***
      DO 420 I=1,5
      CALL TBEKP(ZZ(I,2),TRAD(I),Z,XLIMIT,4,INDX,128,6,ICHK,NTEST)
  420 TRAD(I)=TRAD(I)/2.
      WRITE(6,341) ZZ $ WRITE(6,341) TRAD
      SUMSQ=0. $ NDN=0
      CALL FLIN(ZZ,5,TRAD,A)
      WRITE(6,341) A
      DO 430 I=15,140
      NDN=NDN+1
      POLYT=A(1)
      DO 440 J=1,4
  440 POLYT=POLYT+A(J+1)*Z(I)**J
      SUMSQ=SUMSQ+(POLYT-XLIMIT(I)/2.)**2
      IF(I/2*2.NE.I) GO TO 430
      WRITE(6,1063) I,Z(I),POLYT
  430 CONTINUE
      SUMSQ=(SUMSQ/NDN)**0.5
      WRITE(6,451) SUMSQ
  451 FORMAT(10X,*RMS ERROR OF FIT =*,1PE14.4)
      WRITE(6,1023)
 1023 FORMAT(5X,*STEP*,7X,*BZ*,5X,*BTOTAL*,7X,*PMAG*,5X,*TEST1*,5X,
     .*BLUDX*,9X,*DR*,9X,*Z*)
      DO 795 J=1,NSTEP
      RAD(J)=A(1) $ DO 700 K=1,4
  700 RAD(J)=RAD(J)+A(K+1)*Z(J)**K
      S=A(2)+2.*A(3)*Z(J)+3.*A(4)*Z(J)**2+4.*A(5)*Z(J)**3
      Y=2.*A(3)+6.*A(4)*Z(4)+12.*A(5)*Z(J)**2
      YPRIM=6.*A(4)+24.*A(5)*Z(J)
      BZ1=BFLUX/(PY*RAD(J)**2) $ BZ(J)=BZ1
      DR=RAD(J)/100. $ BRAR=0. $ BTOTAL=0.
      DO 710 IR=1,100
      ARE=(IR-0.5)*DR
      BR=(BFLUX/PY)*S*ARE/RAD(J)**3
      BTOTAL=BTOTAL+2.*PY*ARE*DR*SQRT(BR**2+BZ1**2)
  710 CONTINUE
      BTOT(J)=BTOTAL/(PY*RAD(J)**2)
      PMAG(J)=BTOT(J)**2/(8.*PY)
```

```
*         [illegible] INTEGRALS
*
      TEST1=-(1.+(RAD(J)/2.)*(Y-3.*S**2/RAD(J))-S**2)
      [illegible]=((3[illegible]/-Y)**2/RAD(J)**4)/(2.*PY)
      DP(J)=[illegible]*TEST1
      [illegible] GO TO 795
      [illegible](6,1076) J,BZ(J),BTOTAL,RAAS(J),TEST1,FLUCON,DP(J)
  795 [illegible]
      [illegible](6,1077)
 1077 [illegible]*,1X,*BFIELD*,7X,*BTOT*,4X,*XLIMITC*,5X,*XX*,3X,
     [illegible]
C         [illegible] MAGNETIC FIELD INTENSITY
      [illegible]
      [illegible]
      XY=1.+.2*([illegible]-DP(I))/DELP
      [illegible]
      [illegible]**0.5*1.1253792
      [illegible]
      [illegible] I,BFIELD(I),BTOT(I),XLIMITC(I),XX,DELP,DP(I),Z(I)
 1075 [illegible]
      [illegible] I,BFIELD(I),XLIMITC(I),DP(I)
  420 [illegible]
      [illegible]
      [illegible]
      [illegible](ZZ(I,2),OPSTAB(I,2),7,DP,4,INDX,12P,6,ICHK,NTEST)
  [illegible](OPSTAB(I,1)-OPSTAB(I,2))
      [illegible]
C
C         PUT TEST HERE FOR OPTEST AND LOOPING
C
      DO [illegible] I=1,[illegible]
 9761 [illegible] (I,1) = OPSTAB(I,2)
      [illegible]
 9762 XLIMIT(I) = XLIMITC(I)
 97[illegible]
      [illegible]
    2 FORMAT(7E11.4)
    3 READ(5,7) XLIM
      [illegible] IHORZ
    7 [illegible].4)
      [illegible]
      [illegible] WAVLE,LABEL
  971 FORMAT(/20X,17H WAVE-LENGTH (CM)=,1PE12.4,20X,8A2)
C
C XLIM IS THE DIAMETER OF THE COLUMN
C
      WRITE (6,972) XLIM,ZLIM,IHORZ
  972 FORMAT(//21X,5HXLIM=,1PE11.4,7X,5HZLIM=,E11.4,38X,19H MIN. LEVELS
     [illegible]
      [illegible]
      LIM72=NSTEP
      [illegible]
   61 WRITE(6,84) LOCK,LKLIM,NBASE
   84 FORMAT(20X,12H RAY OFFSET ,I3,8X,6H STEPS,3HTO ,I4,5HSTEPS,20X,
     [illegible],I3//)
  778 [illegible]
      [illegible]=0.0
```

```
                      AMU=1.00
230                   THETAR=0.0
C
C     BEGINNING OF MAIN LOOP FOR A GIVEN MODEL - STMT 92
C
                   92 CONTINUE
235                   TAUPH1=TAUPH2=TAUPH3=TAUPH4=0.0
                      TRANSP=0.0
                      DX=0.05
                      DO 77 N=1,NSTEP
                   77 XSIMP(N)=B(TP(N))*EXP(-TAUP(N)/AMU) *TAUP(N)
240                   WRITE(6,2) XSIMP
                      CALL SIMPSN(Y,XSIMP,DX,NSTEP)
                      TRANSP=Y
                      IF(AMU-1.0-5) 86,86,87
                   86 PHIP=TRANSP
245                   PHIP=TRANSP/TRANS1
                      WRITE(6,75) TRANS1,TRANSP,PHIP
                   75 FORMAT(/4X,26HPHOTOSPHERIC I(0,0)=,1PE11.4,3X,15HFACULAR I(0,0)=,
                     1 E11.4,3X,13HFACULAR PHI(0)=,0PF11.4/)
                   87 PHIP=TRANSP/TRANS1
250                   AMU=10.**ANGL
                      THETAR=ACOS(AMU)
                      WRITE(6,88) TRANSP,PHIP,AMU
                   88 FORMAT(///25X,13H PHOTOSPHERIC//40X,10H INTENSITY,14X,4H PHI,10X,
                     1  10H COS THETA/40X,1PE11.4, 7X,0PF11.4, 7X,F9.4///)
255                   WRITE(6,15)
                   15 FORMAT(20X,9HLEVEL,4X,13HHEIGHT OF RAY,5X,9HUPPER PH,3X,7HFACULAR,
                     1   10X,9HLOWER PH,5X,3HTAU/4X,9HLI471,3X,9HLIMZ2,3X,6HOF RAY,2X,
                     2  15HABOVE ATMOSPHERE,3X,9HINTENSITY,4X,9HINTENSITY,4X,9HINTENSITY
                     3,2X,9HIN FACUL,5X,9HCONTRAST//)
260                   TNOT=(1./AMU**2-1.)**.5
C
C     INNER LOOP FOR GIVEN MODEL
C
                   502 CONTINUE
265                   STEP=.01
                      TRANS=0.0
                      TAUP=0.0
                      SUMY=0.
                      IF(1.-AMU-1.E-10) 6,6,4
                    4 DO 12 N=1,NSTEP
                      K=N
                      IF(ALOG10(TAUP(N))-ALOG10(AMU)-.01) 12,13,13
                   12 CONTINUE
                   13 KDOK=NN+LOOK
275                   IF(N-NSTEP.LT.1) 200,199
                  200 WRITE(6,201)
                  201 FORMAT(/*REACHED TOP OF ATMOSPHERE*/)
                      GO TO 12
                  199 ZBASE=Z(KDOK)
280                   HTAUI=Z(NBASE)-ZBASE
                  202 FORMAT(6H KDOK=,I3,11H NEW ZBASE=,1PE12.4,33H HEIGHT OF RAY ABOVE
                     1PHOTOSPHERE=,0PF12.4)
                      DO 16 N=1,NSTEP
                      ZP(N)=ZP(N)-ZBASE
283                   16 Z(N)=Z(N)-ZBASE
```

THE ASTROPHYSICAL JOURNAL, 242:L15–L18, 1980 November 15

VARIATIONS IN THE SOLAR CONSTANT DUE TO SOLAR ACTIVE REGIONS

G. A. CHAPMAN
San Fernando Observatory and Department of Physics and Astronomy, California State University, Northridge
Received 1978 July 25; accepted 1980 August 14

ABSTRACT

Solar activity is expected to affect the solar constant at some level. Recent observations and data analysis show the amount of variation to be expected from active regions, faculae, and sunspots on the apparent solar brightness. It is concluded that the maximum effect is about 20 times greater for sunspots than for faculae per unit area. Because facular areas are 25–30 times those for sunspots, the effect on the solar constant of faculae and sunspots is approximately equal and opposite, being typically in the neighborhood of 40–100 parts per million (ppm), but on occasion able to reach over 200 ppm. The issue of energy balance is not discussed here, for it requires further data analysis as well as information on the facular and sunspot limb darkening.

Subject headings: Sun: activity — Sun: faculae — Sun: sunspots

I. INTRODUCTION

Sunspots and faculae are the most easily seen effects of solar active regions. Sunspots are best seen in the central regions of the solar disk, whereas faculae are best seen near the solar limb. Because their intensities are different functions of viewing angle, sunspots and faculae could cause small changes in the solar constant, even if the solar luminosity is constant. Abbot (1958) claimed to have detected a 2% decrease in the solar constant coinciding within a few days of the central disk passage of a large sunspot. Such a large effect seems unlikely, as was pointed out by Smith and Gottlieb (1974). The analysis of Smithsonian and *Mariner 6* and *7* data by Foukal, Mack, and Vernazza (1977) showed that, down to a level of 3×10^{-4}, sunspots should have an imperceptible effect on the solar constant. They also found that faculae should cause an increase in the solar constant at a level of approximately 7×10^{-4}, although this result was not statistically significant at the 2σ level. More recently, Foukal and Vernazza (1979) found in correlation analysis a clear indication of solar activity in the Smithsonian data at a level of about 3×10^{-4} due to the presence of faculae and sunspots.

There have been very few observations of the spatially integrated excess brightness of sunspots and faculae. Recently, Livingston (1978*a*) has inferred a possible increase in the solar brightness due to faculae of about 3×10^{-3}($\Delta T \approx +4$ K). This increase was inferred from seeing two peaks, in his spectral-line monitor program, separated by about 14 days. These peaks were correlated with faculae at opposite limbs. However, with increased solar activity, from 1975 through 1977 there appeared to be a global cooling trend, $\Delta S/S \approx -5 \times 10^{-3}$. Livingston (1978*b*) reports that with increasing activity the facular modulation has become less clear. To determine more clearly the effects of faculae and sunspots on the solar brightness one needs direct measurements of these features resolved against the solar disk.

The data presented here have been converted into solar constant variations by assuming that the brightness variations associated with sunspots and faculae are not compensated by changes in the energy output of the quiet Sun. Several possibilities exist for the redistribution (caused by solar activity) of the flow of heat. First, there could be a steady state flow in which the flux blocked by sunspots is instead radiated away by faculae. Because of their different center-to-limb contrast behavior, one would expect to see a change in the solar constant even though the solar luminosity was constant. Second, the convection zone could be a reservoir for storing heat blocked by sunspots or releasing heat for radiation by faculae. In this case the solar constant would change, and some of that change (though not necessarily all) would correspond to a change in luminosity. Finally, the energy blocked by sunspots could reappear "promptly" as increased radiation from the surrounding photosphere. In the case of faculae this prompt readjustment in the heat flux from the quiet Sun would result in a change in the solar constant since faculae will redistribute the direction of their radiation.

In this *Letter* we specifically assume the first proposition. Under the other possibilities there should be variations in the solar constant due to solar activity, but their quantitative determination by areal photometry becomes considerably more difficult.

II. THE OBSERVATIONS

a) Instrumental Techniques

The Extreme Limb Photometer (ELP) has been described elsewhere (Chapman 1975), but we will review the description. Observations are obtained of faculae and sunspots by sweeping across them with a rotary scanner whose $3'' \times 38''$ slits are aligned along radii. The data are normalized by the central intensity of the solar disk. Measurements in 1975 were often obtained in five colors, 0.43, 0.52, 0.66, 0.79, and 1.01 μm, and the color dependence of faculae was described by

Chapman and McGuire (1977). Most measurements from 1974 and 1975 were obtained in the green ($\lambda = 0.52\ \mu$m) with a bandpass of 0.08 μm. In § III we discuss bolometric corrections to the monochromatic changes in brightness reported here.

When an active region was at or near the limb, the ELP was centered on the solar disk so that the apertures scanned the limb. For active regions away from the limb, the ELP was moved so that one aperture mapped out the active region as seen on real-time readouts. The sensitivity of the photometer to a localized brightness change when the photometer was Sun centered was about 1×10^{-5} as a fraction of the mean disk brightness. The smallest value observed for a localized brightness change, at $\lambda = 0.52\ \mu$m, was 6×10^{-3} averaged only over the observed facular area.

b) The Data

A number of sunspots and facular regions were observed during 1974 and 1975. A selection from that data set is collected here. The photometer signal is a portion of an azimuthal scan which contains 2048 steps for 360° of rotation. The simplest signal to analyze is that for Sun-centered operation when the apertures are made to scan the extreme solar limb. The integrated intensity excess or deficit is given by

$$\frac{\Delta I}{\langle I \rangle} = \int_{\phi_1}^{\phi_2} \int_{r_i}^{r_0} (I - \langle I \rangle) dr d\phi / \langle I \rangle (r_0 - r_i) , \quad (1)$$

where r_i is the inner edge of an aperture, r_0 is the outer edge of the solar limb, and $\langle I \rangle$ is the mean value of the brightness of the quiet Sun (no active region). The integration is performed only over the active region. Since $I(\phi)$ is digital, we approximate the integral by the sum

$$\frac{\Delta I}{\langle I \rangle} = \frac{2\pi}{2048} \frac{\sum_i \Delta I_i}{\langle I \rangle} , \quad (2)$$

where $\Delta I_i = I_i - \langle I \rangle$. The factor $2\pi/2048$ converts the result into radian measure. The fractional change in the solar brightness $\Delta B/B$ is approximately given, neglecting $(\delta/R)^2$, by

$$\frac{\Delta B}{B} = \frac{l}{\pi R} \frac{\langle I \rangle}{\bar{I}} \frac{\Delta I}{\langle I \rangle} , \quad (3)$$

where $\bar{I}$ is the mean brightness of the solar disk (Allen 1973), $\delta = r_0 - r_i$, l is the aperture length, and R is the solar radius. We can express a change in solar brightness in terms of an apparent solar oblateness induced by faculae. Apparent oblateness was given in Figure 5 of Chapman (1975) in units of quadrants. To express these values in terms of solar brightness changes we use

$$\frac{\Delta B}{B} = \left[\frac{1}{2} \frac{I_i}{\langle I \rangle} \left(\frac{\langle I \rangle}{I_0} \times \frac{I_0}{\bar{I}}\right) \frac{l}{\delta}\right] \left(\frac{\Delta r}{r}\right)_{\text{quad}} . \quad (4)$$

A typical value of the quantity in brackets for the 1974 observing season was 0.53. The largest brightness change from 1974 was approximately 6×10^{-5}.

To map out all of an active region, away from the limb, requires moving the telescope between sets of scans by the length of the scanning aperture 38″. Several active regions were mapped by sets of scans during 1975, but the analysis has not been completed; hence most of the data discussed are from Sun centered observations. Scans containing sunspots have been only partially analyzed.

A typical example of a sunspot scan will be discussed. A large single sunspot, Mount Wilson 19148, was scanned on 1974 August 9. This sunspot had an area of 3.10^{-4} of a hemisphere, according to the *Solar Geophysical Data* and was not far from the center of the solar disk. We measured a mean contrast of −0.221 over an interval of 20 steps of the ELP. Converting this contrast to an apparent change in brightness of the solar disk, we have

$$\left(\frac{\Delta B}{B}\right)_s = \frac{\Delta I}{\langle I \rangle} \times \frac{\langle I \rangle}{\bar{I}} \times \frac{A_{\text{ELP}}}{\pi R^2} . \quad (5)$$

The quantity $\langle I \rangle / \bar{I} = \langle I \rangle / I_0 (I_0 / \bar{I})$, where $\langle I \rangle / I_0 = 0.975$ and $I_0/\bar{I} = 1/0.800$ at $\lambda = 0.55\ \mu$m (Allen 1973). The area encompassed by 20 steps near disk center is $A_{\text{ELP}} = 1.19 \times 10^{19}$ cm^2. We thus have from equation (5):

$$\left(\frac{\Delta B}{B}\right)_s = -2.12 \times 10^{-4} . \quad (6)$$

An estimate of $\Delta B/B$ based on typical sunspot brightness and the above-mentioned area of 3.10^{-4} gives $\Delta B/B = -1.1 \times 10^{-4}$, a factor of 2 less than that of equation (6).

Table 1 presents the apparent change in the solar brightness at $\lambda = 0.52\ \mu$m due to the presence of

TABLE 1

SOLAR BRIGHTNESS CHANGES DUE TO ACTIVE REGIONS NEAR THE LIMB IN 1975

Date	$\Delta B/B$ (10^{-6})	McMath No. (13000+)	McMath Area[a]
	July		
14.....	37.0	766, 767	2600, 500
15.....	28.5	766, 750	3000, 2900
	August		
9.....	27.4	796	700
10.....	88.7	796, 786	1500, 4800
11.....	28.9	786	2000
13.....	11.2	790	4500
14.....	63.2	790	4800
15.....	37.5	790	...
16.....	18.5	808, 790	8000, 1000
25.....	44.2	820	900
26.....	28.6	820	2500
27.....	13.4	820	2000
28.....	25.2	826	800
29.....	45.1	826, 818	...
30.....	94.7	826, 818	...

[a] In millionths of a hemisphere.

faculae at the limb. The variations are all positive, even though sunspots are sometimes present, because at the limb faculae are usually more visible than sunspots.

The results are the sum of the two ELP apertures and on some days are the combination of two active regions at opposite limbs. The outer aperture covered from the sky to 16″ inside the limb, and the other covered the disk from 16″ to 51″ inside the limb. The largest brightness change is on 1975 August 30, with a change of 9.5×10^{-5}. The mean brightness excess for the 15 days indicated in Table 1 is $(39.5 \pm 6.4) \times 10^{-6}$.

Table 2 gives apparent brightness changes expected from a sunspot observed on three successive days, 1975 July 18, 19, and 20. The sunspot was Mount Wilson 589, which was embedded in the active region McMath 13766. For the three successive days, the mean brightness change was $-(140.6 \pm 1.7) \times 10^{-6}$, where the uncertainty is the standard deviation of the mean. The area for these same three days was 2.20^{-4} (*Solar Geophysical Data* 1975). It is interesting that on July 20 the brightness change was independent of the area scanned. This observation needs to be confirmed, but it may permit one to set limits on the redistribution of energy in the quiet photosphere around the sunspot.

III. DISCUSSION

The changes in apparent solar brightness are for a wavelength band centered at 0.52 μm. We would like to know the effects of this brightness change on bolometric measurements of the solar output. For this purpose we have calculated the range of possible corrections to the monochromatic brightness changes by considering the bolometric and monochromatic contrast of representative blackbodies at 4000 K and at 6400 K with respect to 5800 K, which represents the quiet Sun. The temperature of 6400 K represents an extreme model for a facular region, whereas 4000 K represents a sunspot (these temperatures are illustrative only). The results are summarized in Table 3. For these temperature ratios, the monochromatic contrast must be decreased by about 14% to give the bolometric contrast. Considering other sources of uncertainty, we consider the uncertainty in these corrections to be of small importance. If the temperatures of faculae or sunspots are closer to the quiet Sun than assumed here, then the bolometric corrections will also be smaller than assumed here. Thus in the absence of any compensating effect, the variations in the solar constant should be approximately 86% of the values of $\Delta B/B$ given in Tables 1 and 2.

TABLE 2

BRIGHTNESS CHANGES DUE TO A SUNSPOT NEAR DISK CENTER (Mount Wilson 589)

Date 1975	File Number	ELP Steps	cos θ	$\Delta B/B$ (10^{-6})	Area[a]
July 18.....	12	32	0.95	−1.39	250
	17	30	...	−1.42	...
July 19.....	13	18	0.98	−1.46	170
	19	18	...	−1.44	...
July 20.....	16	40	0.97	−1.36	250
Spot only[b]...	16	13	0.97	−1.37	...

[a] *Solar Geophysical Data* in millionths of a hemisphere.

[b] 38″ × 38″ square area including spot.

TABLE 3

MONOCHROMATIC AND BOLOMETRIC CONTRASTS RELATIVE TO A BLACKBODY AT 5800 K AND 0.52 MICRONS

T(K)	$(\Delta I/I)_\lambda$	$(\Delta I/I)_{bol}$	Corr. Factor[a]
6400 ...	+0.571	+0.483	0.846
4000 ...	−0.884	−0.774	0.876

[a] Not a standard bolometric correction.

We have referred to changes in solar brightness rather than luminosity in order to avoid implying that the actual solar output changes with time. The change in solar luminosity must be inferred from knowledge of the radiative energy balance between sunspots and faculae. If there were energy balance between sunspots and faculae, we would still expect to see changes in the solar brightness because of their different center-to-limb contrasts.

In order for there to be no brightness change due to active regions would require the quiet Sun to redistribute the energy blocked by sunspots with no time delay. This energy would have to be emitted with the same angular dependence as that of the quiet photosphere and could not look like faculae.

From a statistical analysis of the Smithsonian data on the solar constant, Foukal and Vernazza (1979) have found a variation due to faculae at a level of about 3×10^{-4}. They also found a possible time lag of about 1 day between the decrease in the solar constant and the appearance of a sunspot, and they discussed the implications of the time lag on the depth of the convection zone.

Thus, from the Abbot-Smithsonian data analyzed by Foukal and Vernazza (1979), it seems likely that there are solar brightness changes. Assuming no change in the quiet Sun, we find that sunspots produce a change in solar brightness of

$$\frac{\Delta B}{B} = 6.2 \times 10^{-1} A_s , \qquad (7)$$

where A_s is the spot area in fractions of a hemisphere. This relation implies that for spot areas of 2×10^{-3} one would expect a brightness deficit of about 1.2×10^{-3}, ignoring the effects of faculae. This value is within the limits set by the *Nimbus* data quoted by Foukal and Vernazza (1979).

Faculae cause a solar brightness excess of

$$\frac{\Delta B}{B} = (3.0\text{–}4.0) \times 10^{-2} A_{\text{plage}} , \qquad (8)$$

where A_{plage} is the plage area in fractions of the hemisphere. The maximum change to be expected, based on large plage areas, is about 1×10^{-3} for facular regions

near the limb. For facular regions near disk center, the brightness excess will be about 10 times less (Chapman and Klabunde 1980; Skumanich, Smythe, and Frazier 1975). The uncertainty in equation (8) is due to incomplete coverage of the larger facular regions. This uncertainty can be narrowed by an analysis of photographs of the active regions.

Considering that faculae and sunspots have opposite effects on the solar brightness, one would estimate that the average effect from both would be about one-half of the extreme, or about ± 5 or 6×10^{-4}. This value is in good agreement with the results of Foukal and Vernazza's (1979) study of the Abbot Smithsonian data.

The question of flux balance will be discussed in a forthcoming paper after further data analysis. Presently, it appears that the flux deficit due to sunspots *may* be balanced by the flux excess of faculae. If true, one still expects to see the brightness variations described here.

The active cavity radiometer on the *Solar Maximum Mission* spacecraft has detected variations in the solar constant of approximately $\pm 3 \times 10^{-3}$ (Willson 1980). These variations are in the range to be expected from solar activity, and it will be desirable to compare such observations with changes caused by faculae and sunspots.

One might ask at what positions on the solar disk do sunspots and faculae make their greatest contributions to brightness changes? The maximum contrast of sunspots is at the disk center (Zwaan 1974) and the maximum contrast of faculae is near the limb. The contribution of an active region depends on this contrast but also on the projected area and the nearby quiet-Sun brightness (cf. eqs. [3] and [5]). The area of an active region depends on μ, and the quiet-Sun brightness varies crudely like μ. We suggest that while sunspots have their maximum contribution at $\mu = 1$, the position where faculae make their maximum contribution is not yet certain. Adapting equation (5), we examine the possible variation of

$$\frac{\Delta I}{\langle I \rangle} \frac{\langle I \rangle}{I} A_{\rm ELP} . \tag{9}$$

A preliminary expression for the first fraction is

$$\frac{\Delta I}{\langle I \rangle} = b(\mu^{-1} - a) , \quad 0 \leq a \leq 1 \tag{10}$$

(Chapman and Klabunde 1980). The second term is composed of

$$\frac{\langle I \rangle}{I_\odot} \frac{I_\odot}{I} , \tag{11}$$

where $\langle I \rangle / I_\odot$ is approximately equal to μ over much of the solar disk. Finally, $A_{\rm ELP}$ is proportional to μ, so that equation (9) is proportional to

$$b\mu^2(\mu^{-1} - a) . \tag{12}$$

If $a = 0$, then faculae contribute most when at disk center ($\mu = 1$). If $a = 1$, then faculae contribute most at $\mu = \frac{1}{2}$, which occurs $\sim 4\frac{1}{2}$ days of rotation from disk center. In support of $a = 1$, we find that faculae are not clearly seen at disk center with the ELP, and sunspots give a large negative contrast. At the limb, the positive facular contrast is seldom equalled or exceeded by the negative sunspot contrast, i.e., facular regions at the limb containing large sunspots usually have a net positive contrast. Based on data obtained in 1979, we suggest preliminary values for a and b of 1 and 0.04, respectively.

I wish to thank T. E. McGuire for his help in acquiring some of the data in 1975. I also thank D. P. Klabunde and A. D. Meyer for data analysis help. This research was supported in part by NASA grants NSG7456 and NSG5330.

REFERENCES

Abbot, C. G. 1958, *Smithsonian Contr. Ap.*, **3**, 13.
Allen, C. W. 1973, *Astrophysical Quantities* (3d ed.; London: Athlone).
Chapman, G. A. 1975, *Proc. 7th Texas Symp. Relativistic Astrophysics* (*N.Y. Acad. Science*, **262**, 481).
Chapman, G. A., and Klabunde, D. P. 1980, in preparation.
Chapman, G. A., and McGuire, T. E. 1977, *Ap. J.*, **217**, 657.
Foukal, P. V., Mack, P. E., and Vernazza, J. E. 1977, *Ap. J.*, **215**, 952.
Foukal, P. V., and Vernazza, J. E. 1979, *Ap. J.*, **234**, 707.
Livingston, W. C. 1978*a*, *Nature*, **272**, 340.
———. 1978*b*, Conf. on Solar and Terrestrial Influences on Weather and Climate, Columbus, Ohio, July 24–28.
Skumanich, A., Smythe, C., and Frazier, E. N. 1975, *Ap. J.*, **200**, 747.
Smith, E. V. P., and Gottlieb, D. M. 1974, *Space Sci. Rev.*, **16**, 771.
Solar Geophysical Data. 1975 (Boulder, Colo.: U.S. Department of Commerce).
Willson, R. C. 1980, Meeting Am. Geophys. Union, Toronto, May 27.
Zwaan, C. 1974, *Solar Phys.*, **37**, 99.

GARY A. CHAPMAN: Department of Physics and Astronomy, California State University, Northridge, CA 91330

PROCEEDINGS

OF

THE JAPAN-FRANCE SEMINAR

ON

SOLAR PHYSICS

EDITED BY

F. MORIYAMA AND J. C. HENOUX

January, 1981

THE MAGNETIC FIELD FLUX IN FACULAR REGIONS

Z. Mouradian[1], G. Chapman[2], S. Dumont[3], Ch. Fang[1,4], Y. Feng[1,5], J.C. Pecker[3]

1 Observatoire de Paris-Meudon

2 California State University, Northridge, USA

3 L.A.T. College de France

4 Université de Nankin, Chine

5 Observatoire de Yunnan, Chine

1. Introduction

The solar magnetic field ($\vec{B}$) is usually studied by observation of the value of the line-of-sight component (B_n), (Harvey, 1977). In the present note we give preliminary results of another approach ; the study of the flux of the line- of-sight component (ϕ) of magnetic structures. Our study is statistical.

2. Data

To carry out this investigation, we used observations taken with the Kitt Peak magnetograph (Pecker et al., 1977). Maps (512" x 450") of B_n were obtained with the FeI λ 868,86 nm line and with an observing aperture of 1" x 1". The spatial resolution was about 1",5 to 2",5. We measured the flux (ϕ) of the magnetic structures limited by the Isogauss 25, where

$$\phi = \int_S B_n \, dS \qquad \text{for } B_n \geq 25 \text{ gauss}$$

The surface (S) of the structures is between 6 and 2000 " x " The experimental error is less than 10 gauss for the given aperture.

3. Results

For each magnetic structure, we measured the flux (ϕ) through the surface (S) and obtained an empirical relation of the forme

$$\log \phi = c + d \log S \qquad (1)$$

The figure shows an example for the center of the solar disk. Two conclusions may be drawn : i) there is no basic difference between the magnetic field in faculae

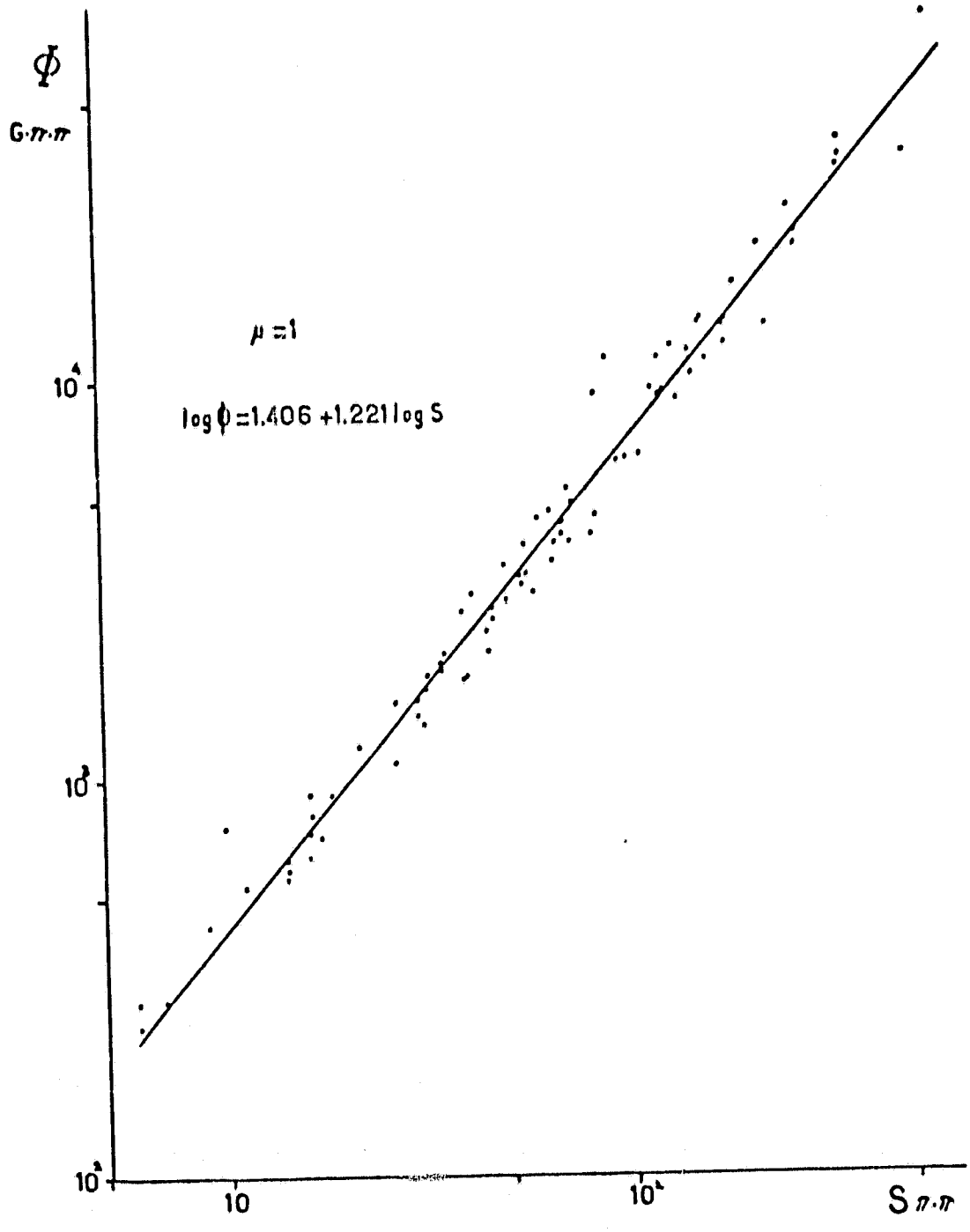
Φ
G·m·m
μ =1
log Φ =1.406 +1.221 log S
10⁴
10³
10²
10
10²
S m·m

and in plages, and ii) a very strong relationship exists between the flux of B_n and the occupied surface.

In our study, we do not take into account sunspots and pores, or peculiar regions such as bright X points, etc.

The relation (1) remains valid over the whole solar disk, only the constants changing :

μ	Δμ	N	c	d	r	σ
1	1 -0.97	83	1.406	1.221	0.992	0.072
0.71	0.88-0.37	79	1.421	1.275	0.984	0.082
0.60	0.71-0.48	45	1.529	1.139	0.990	0.063
0.35	0.47-0	27	1.488	1.164	0.992	0.050

In the table, N represents the number of measured structures, r is the correlation coefficient and 6 is the standard deviation.

Two corrections can be applied to the relation (1) ; the first is a correction for the seeing influence and the second is for the influence of choice of the boundary of the structure, i. . $B_n \geq 25$ gauss, instead of the isogauss curve $B_n = 0$.

The effect of the image quality is studied in two successive observations of the same region, one with good seeing and the other with bad seeing. The results show a "tilt" of the logarithmic relationship between ϕ and S, when the seeing is bad.

IQ	N	c	d	r	σ
good	63	1.399	1.228	0.997	0.061
bad	90	1.397	1.317	0.987	0.087

From the relation (1) and an examination of the choice of contours, we see an important change in the value of the c constant. The relation (1) becomes :

$$\log \phi_c = 0.34 + 1.44 \log S \qquad (2)$$

This is the true relationship between ϕ and S for the center of the solar disk. From the relation (2) we can compute the flux through a surface of 5" x 5" as done

by Wiehr (1979) for the Fe I λ 525,02 nm line. In the present study, we obtained a value of 1.2 10^{18} Mx, which is half of the value obtained by Wiehr. This discrepancy can be explained by the fact that the two sets of observations were performed for different lines.

We would also point out that the Meudon observations give the same relation (1) and same constants, even when the technique of observation and the spectral lines used are entirely different.

REFERENCES

Harvey, J. : 1977, Highlights in Astronomy, Vol. 4, Part II, 223.

Pecker, J.C., Dumont, S., Mouradian Z., Chapman, G.A. : 1977, Proceeding of the November 7-10, 1977 OSO-8 Workshop, Univ. of Colorado, 172.

Wiehr, E. : 1979, Astron. Astrophys. 73, L19.